Cell. Mol. Life Sci. (2010) 67:1881–1894
DOI 10.1007/s00018-010-0298-6

Cellular and Molecular Life Sciences

RESEARCH ARTICLE

Syndecan-4 promotes cytokinesis in a phosphorylation-dependent manner

Aniko Keller-Pinter · Sandor Bottka · Jozsef Timar · Janina Kulka · Robert Katona · Laszlo Dux · Ferenc Deak · Laszlo Szilak

Received: 19 June 2009 / Revised: 18 January 2010 / Accepted: 1 February 2010 / Published online: 14 March 2010

Abstract During mitosis, cells detach, and the cell–matrix interactions become restricted. At the completion of cytokinesis, the two daughter cells are still connected transiently by an intercellular bridge (ICB), which is subjected to abscission, as the terminal step of cytokinesis. Cell adhesion to the matrix is mediated by syndecan-4 (SDC4) transmembrane heparan sulfate proteoglycan. Our present work demonstrated that SDC4 promotes cytokinesis in a phosphorylation-dependent manner in MCF-7 breast adenocarcinoma cells. The serine179-phosphorylation and the ectodomain shedding of SDC4 changed periodically in a cell cycle-dependent way reaching the maximum at G2/M phases. On the contrary, the phospho-resistant Ser179Ala mutant abrogated the shedding. The phosphorylated full-length and shed remnants enriched along the mitotic spindles, and subsequently in the ICBs, however, proper membrane insertion was necessary for midbody localization. Expression of phosphomimicking Ser179Glu SDC4 resulted in incomplete abscission, whereas expression of the phospho-resistant SDC4 led to giant, multinucleated cells.

Keywords Syndecan-4 · Phosphorylation · Shedding · Cytokinesis · Intercellular bridge · Midbody · Multinucleation

Electronic supplementary material The online version of this article (doi:10.1007/s00018-010-0298-6) contains supplementary material, which is available to authorized users.

A. Keller-Pinter · J. Timar · J. Kulka
2nd Department of Pathology, Semmelweis University, Budapest, Hungary

A. Keller-Pinter · L. Dux
Department of Biochemistry, Faculty of General Medicine, University of Szeged, Szeged, Hungary

S. Bottka
Institute of Plant Biology, Biological Research Center of the Hungarian Academy of Sciences, Szeged, Hungary

R. Katona
Institute of Genetics, Biological Research Center of the Hungarian Academy of Sciences, Szeged, Hungary

F. Deak
Institute of Biochemistry, Biological Research Center of the Hungarian Academy of Sciences, Szeged, Hungary

L. Szilak
Szilak Laboratories Bioinformatics and Molecule-Design Ltd., Szeged, Hungary

L. Szilak (✉)
Savaria University Center, Institute of Biology, Western Hungarian University, Szombathely, Hungary
e-mail: laszlo.szilak@gmail.com

L. Szilak
Department of Medical Biochemistry, Semmelweis University, Budapest, Hungary

Introduction

Following nuclear division, cells divide into two daughter cells by a process known as cytokinesis. In the dividing cells, an invagination of the plasma membrane (cleavage furrow) is created by an actomyosin-based structure, which proceeds until the cytoplasm is constricted to a narrow intercellular bridge (ICB). The ICBs contain parallel arrays of spindle microtubules, which are connected through a dense structure defined as midbody connecting the prospective daughter cells. In the final stage of the process, termed abscission, the ICBs are ultimately resolved and the

two cells separate [1–3]. Proteins involved in cytokinesis and several essential components of the midbody have been recently identified by functional proteomic approach [4]. However, a complete survey of the midbody composition is lacking largely impart to its transient nature [5, 6].

Growing cells keep tight contact with the extracellular matrix (ECM). During cell division, adherent cells reorganize their adhesive interactions with the ECM; at the early phase of mitosis cells detach and round up, after executing cytokinesis they start reattaching and spreading. In L929 and NIH3T3 cells, the abscission was influenced by the concentration of fibronectin, yet a direct mechanism was not suggested [2]. Stable cell–matrix contacts (focal adhesions) organized on fibronectin require interactions between the heparin-binding domain of fibronectin and heparan sulfate provided by syndecans (SDCs) [7–9].

Syndecans constitute a family of four transmembrane heparan sulfate proteoglycans [10]. They share uniform structure: a divergent extracellular domain (ectodomain) containing glycosaminoglycan attachment sites for heparan sulfate [11, 12], a conserved one-span transmembrane domain and a short cytoplasmic domain representing several protein-interacting sites. It is generally accepted that heparan sulfate-mediated binding of a wide variety of extracellular ligands is central to syndecan functional activity, therefore syndecans are considered as co-receptors of the primary signaling receptors [13]. Among the family members, only syndecan-4 is selectively enriched in focal adhesions and can transmit signals via its cytoplasmic domain [7, 14]. The variable (V) region of the cytoplasmic domain of syndecan-4 binds phosphatidylinositol (4, 5)-bisphosphate (PIP2) and activates protein kinase C alpha (PKCα). The phosphorylation of the only serine of the cytoplasm (Ser179 in human syndecan-4) reduces the PIP2 binding affinity and consequently the super-activation of PKCα [15–17].

The extracellular domains of syndecans (similarly to other transmembrane proteins) can be released from the cell surface by endogenous proteolytic cleavage in a process known as ectodomain shedding [18]. Hitherto, the studies of syndecan shedding mostly focused on the ectodomain [19], the fate of the cytoplasmic remnant is completely unknown [20].

In the present study, the role of syndecan-4 was studied in the cytokinesis of MCF-7 breast adenocarcinoma cells. During mitosis, the distribution of syndecan-4 was monitored and found to be co-localized with centrosomes and mitotic spindles, accumulated in the spindle midzone, and subsequently in the ICB. Mutational analysis of the regulatory cytoplasmic Ser179 of syndecan-4 revealed that the phosphoresistant Ala mutant was absent while the phosphomimetic Glu mutant was enriched in the ICBs. Monitoring of the ectodomain-shed syndecan-4 remnant we found that the phosphorylated shed remnant abundantly distributed in the cytoplasm. Phosphorylation and shedding of SDC4 was elevated after the S1 phase, reaching the maximum at the G2/M phases whereas shedding of Ser179Ala mutant was abrogated. The expression of the Ser179Glu mutants frequently resulted in incomplete abscission and elongated ICBs, while the Ser179Ala led to the development of giant, multinucleated cells, emphasizing the role of syndecan-4 in the regulation of cytokinesis.

Materials and methods

Cell culture, human syndecan-4 constructs

MCF-7 human breast adenocarcinoma cells obtained from ATCC were cultured in DMEM:F12 medium (Cambrex, Walkersville, MD, USA) containing 10% fetal bovine serum (Gibco, Bethesda, MD, USA). The C2/7 myoblast cell line originated from mouse skeletal muscle [21] was propagated in DMEM supplemented with 10% fetal bovine serum (Gibco) and antibiotics.

The human syndecan-4 cDNA was isolated and cloned into pCMV vector (Clontech, Heidelberg, Germany) (wt-SDC4). The green fluorescent protein (GFP) tag was inserted at the position of 131 of the syndecan-4 amino acid sequence (wt-SDC4-GFP). The Ser179 syndecan-4 was mutated to Ala (Ser179Ala) or Glu (Ser179Glu) by PCR-based method. The shorter forms (DEGE, signal-DEGE) of syndecan-4 were generated from the full-length Ser179Glu version by deletion of the upstream segment from GFP. MCF-7 cells were transfected by the plasmids of interest with FuGene6 transfection reagent (Roche Diagnostics, Mannheim, Germany) according to the manufacturer's instructions. For stable expression, the transfected cells were selected in medium supplemented with 500 μg/ml G418 (Cambrex) and maintained in 200 μg/ml G418.

Immunofluorescence microscopy

Rabbit antiserum to the ectodomain of syndecan-4 (Invitrogen/Zymed Corporation, Carlsbad, CA, USA), goat antiserum to the cytoplasmic domain of syndecan-4, goat (sc-16852) and rabbit (sc-22252-R) antisera to the phospho-Ser179-syndecan-4 and mouse monoclonal anti-alpha-tubulin antibody (all from Santa Cruz Biotechnology, Santa Cruz, CA, USA), mouse anti-TGN38 (*trans* Golgi network protein 38) antibody (BD Biosciences, Franklin Lakes, NJ, USA) were used at appropriate dilutions. F–actin was visualized with TRITC-conjugated phalloidin (Sigma–Aldrich). Hoechst 33258 (Sigma–Aldrich) staining was used to label nuclei. For immunofluorescence, the primary antibodies were detected with Cy3-conjugated Fab

fragment of donkey anti-mouse IgG, Cy3-conjugated Fab of donkey anti rabbit IgG, Cy3-conjugated Fab of donkey anti goat IgG, Cy2-conjugated Fab of donkey anti goat IgG and Cy2-conjugated Fab of donkey anti-rabbit IgG secondary antibodies (Jackson ImmunoResearch Laboratories, West Grove, PA, USA).

All reagents were diluted with phosphate-buffered saline (PBS). Cells grown on glass coverslips coated with 10 μg/ml fibronectin (Sigma–Aldrich) were fixed for 5 min with 4% paraformaldehyde at 37°C, permeabilized with 0.1% Triton X-100 for 5 min, and were incubated for 30 min at room temperature with primary antibodies diluted in 1% bovine serum albumin (Sigma–Aldrich), then were washed three times with PBS, incubated with secondary antibodies in 1% BSA for 20 min at room temperature. After Hoechst nuclear staining, the coverslips were mounted with Fluorescent Mounting Medium (DAKO, Glostrup, Denmark). Images were captured with Zeiss Axio Imager microscope, Nikon Eclipse 600 microscope equipped with Spot RT Slider camera or Bio-Rad MRC-1024 (Bio-Rad, Richmond, CA, USA) confocal microscope. Images were analyzed using Adobe Photoshop, version 8.

Immunoblot and peptide competition assay

Cells grown to 70% confluence were detached with 0.02% EDTA in PBS, centrifuged (2,000 rpm for 5 min at 4°C), washed twice with PBS, and were lysed in buffer containing 25 mM HEPES pH 7.5, 150 mM NaCl, 1% Igepal CA-630, 10 mM $MgCl_2$, 1 mM EDTA, 1 mM NaF, 1 mM Na-orthovanadate and protease inhibitor cocktail (Sigma–Aldrich). After centrifugation at 13,000 rpm for 4 min at 4°C, the supernatants were separated by SDS-PAGE, blotted to PVDF membrane (Millipore, Billerica, MA, USA), and reacted with primary antisera followed by HRP-conjugated secondary antibody purchased from DAKO (Glostrup, Denmark). Peroxidase activity was visualized by the ECL procedure (GE Healthcare, Chalfont St Giles, UK).

Peptide competition assay was performed with 1:1,000 diluted anti-P-SDC4 antibody and increasing amount of phospho-syndecan-4 peptide provided by the supplier (Santa Cruz Biotechnology).

Flow cytometry

The collected cells were washed once with PBS, resuspended in PBS, and fixed by addition of ice-cold 96% ethanol to 70% final concentration. The fixed cells were pelletted by centrifugation (at 2,000 rpm for 10 min), then resuspended in 500 μl of PBS containing 40 μg/ml propidium iodide and 50 μg/ml RNaseA. After 30 min incubation at room temperature, flow cytometry was performed on the Becton & Dickinson FACS Calibur and the data were analyzed by ModFit software.

Cell synchronization and protease inhibition

MCF-7 cells expressing wt-syndecan-4 were synchronized at the G1/S boundary. The medium was removed from exponentially growing cells in 10-cm plastic dishes and was replaced with medium containing 1.5 mM hydroxyurea for 16 h. At selected times after removing the hydroxyurea-containing media, the cells were prepared for flow cytometry or an equal number of cells was lysed in buffer as described above for immunoblot analysis.

For protease inhibition, the cells expressing wt-SDC4-GFP were synchronized with 1.5 mM hydroxyurea for 16 h. After removal of hydroxyurea the cells were incubated with 50 μM broad spectrum metalloproteinase (MMP) inhibitor GM6001 (Millipore) for 6 h, lysed and analyzed by SDS-PAGE followed by immunoblotting.

Cellular fractionation

The 70% confluent cultures of DEGE and signal-DEGE expressing cells were detached, centrifuged (2,000 rpm for 5 min at 4°C) and after washing twice with PBS, the cells were lysed in a buffer containing 100 mM Pipes pH 7.3, 100 mM KCl, 3.5 mM $MgCl_2$, 3 mM NaCl supplemented with 1 mM NaF, 1 mM Na-orthovanadate and protease inhibitor cocktail (Sigma–Aldrich). Homogenates were centrifuged at 10,000 rpm for 5 min to pellet nuclei, and supernatants were then ultracentrifuged at 120,000 × *g* (Sorvall S120-AT2 rotor) for 60 min at 4°C to sediment membrane fraction. The cytosol-containing supernatant was removed and the crude membrane pellet was gently washed with lysis buffer. Membrane fractions were resuspended in lysis buffer in the original volume. Equal volumes of both fractions were analyzed by SDS-PAGE followed by immunoblotting with mouse monoclonal anti-GFP antibody (Invitrogen/Zymed Corporation, Carlsbad, CA, USA).

Results

Phospho-syndecan-4 is associated with the mitotic spindle

Syndecans were previously detected along the mitotic spindle during mitosis by indirect fluorescent immunocytochemistry [22]. We were interested in the nature of the in vivo localization of SDC4 particularly at the mitotic phase of MCF-7 human adenocarcinoma cells.

The expression level of the endogenous SDC4 was rather weak in MCF-7 cells tested on immunoblot (Fig. 1a1) and immunofluorescence (Fig. 1a2), thus it was increased by expression of wt-SDC4. To do so, the full-length human SDC4 cDNA was inserted into pCDNA downstream of a CMV promoter and stably transfected MCF-7 line was generated. The expression level of SDC4 in transfected MCF-7 cells was increased but it did not exceed the endogenous level of C2/7 cells (Fig. 1a1). This arrangement provided a similar expression level of the different constructs of SDC4 (see later).

The distribution of SDC4 was examined by indirect fluorescent immunocytochemistry with antibodies to the extracellular domain (anti-SDC4-ecto), cytoplasmic domain (anti-SDC4-endo) and cytoplasmic domain phosphorylated on Serine 179 (anti-P-SDC4). The localization of SDC4 was characteristic mostly in the plasma membrane, perinuclear region and in the Golgi network of interphase cells visualized by anti-SDC4-ecto antibody staining (Fig. 1b–d) that was in accordance with other observations [23–26]; whereas distribution of the cytoplasmic domain visualized by immunostaining with anti-SDC4-endo or anti-P-SDC4

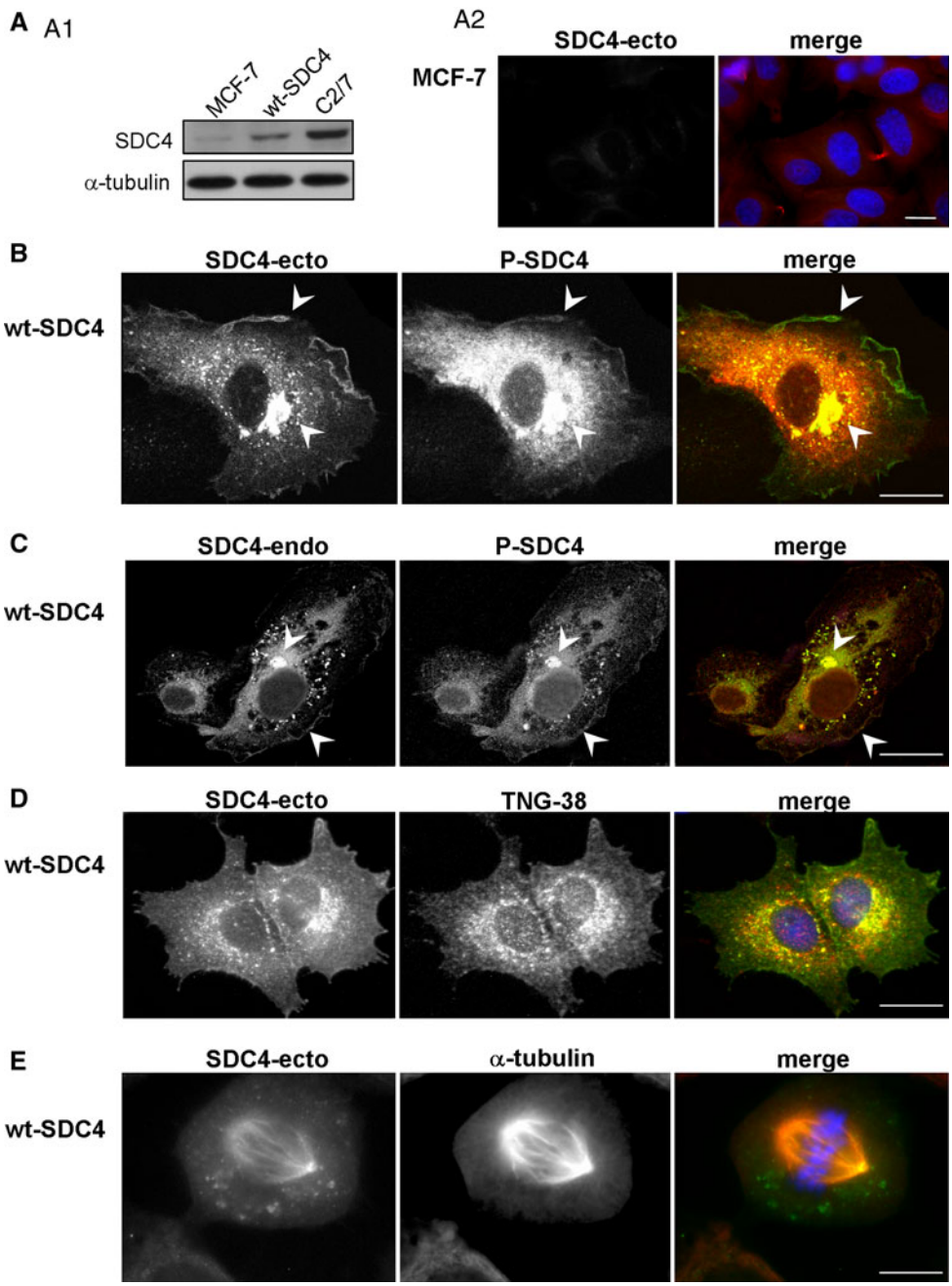

Fig. 1 Intracellular localization of syndecan-4. Lysates of non-transfected MCF-7 cells, wt-SDC4 expressing MCF-7 cells and C2/7 myoblasts were subjected to SDS-PAGE, blotted and developed with anti-SDC4-ecto antibody; anti-α-tubulin antiserum was used as a loading control (**a1**). Non-transfected MCF-7 cells were stained by anti-SDC4-ecto (*green*) and anti-α-tubulin (*red*) antisera (**a2**). Distribution of SDC4 was visualized by confocal microscopy (**b**, **c**). Double immunostaining with anti-SDC4-ecto and anti-P-SDC4 (sc-16852) (**b**) antisera; and anti-P-SDC4 and anti-SDC4-endo (**c**) antisera highlighted distinct patterns in interphase cells. SDC4 was observed mostly in the plasma membrane and in the Golgi vacuoles. To confirm the presence of SDC4 in the Golgi network, double immunostaining was applied with anti-SDC4-ecto (*green*) and anti-trans Golgi network 38 (TGN38, *red*) antibodies (**d**). Previous data indicated that SDC4 localized along the mitotic spindles [22], to validate this MCF-7 cells expressing wt-SDC4 were immunostained with anti-SDC4-ecto (*green*) and anti-α-tubulin (*red*) antibodies (**e**). Nuclear staining was *blue* (Hoechst); *scale bars* represent 20 μm

antisera showed different pattern (Fig. 1b, c). The signal of the cytoplasmic domain was abundantly present in the cytoplasm and overlapped with the signal of the ectodomain mostly at the Golgi vacuoles and in the plasma membrane. Control immunostaining with the secondary antibodies was shown in Suppl. Fig. 1a.

Previously published data demonstrated that a significant amount of phosphorylated syndecan-4 could be detected in cells [27], but its distribution was not studied. Thus, the pattern of phosphorylated syndecan-4 was examined by indirect immunofluorescence microscopy with anti-P-SDC4 and compared to that of anti-SDC4-endo antibody. The two patterns were similar to each other showing enrichment mostly in the Golgi vacuoles and in the nuclei (Fig. 1).

The distribution of wt-SDC4 was monitored in mitotic cells with anti-SDC4-ecto antibody (Fig. 1), too, as it was described previously [22]. SDC4 was detected with the MTOCs and along the mitotic spindle visualized by anti-α-tubulin antibody staining (Fig. 1e).

We studied in detail the distribution of phospho-SDC4 through the phases of mitosis (Fig. 2a–e). The immunostaining revealed that the phospho-SDC4 was co-localized with the microtubule-organizing centers (MTOCs) since they began to separate from the early prophase until anaphase. As mitosis progressed, phospho-syndecan-4 was distributed along the mitotic spindle and accumulated in the spindle midzone from metaphase, represented as dots at the equatorial plane (Fig. 2b, c). In the late telophase phospho-syndecan-4 was enriched in the cleavage furrow (Fig. 2d) and subsequently in the ICBs (Fig. 2e). Importantly, the midbody was not immunoreactive for anti-P-SDC4 (Fig. 2e).

Since the staining patterns of the anti-SDC4-ecto and anti-P-SDC4 antibodies were different from each other (Fig. 1) in interphase cells, anti-SDC4-ecto antibody staining was also applied in dividing cells. The immunostaining could visualize the ICBs, and the midbodies, as well (Fig. 2f). Next, we were going to unravel the nature of the SDC4 enrichment in the midbody region.

Only the Ser179Glu syndecan-4 is localized at the midbody; the Ser179Ala mutant is missing from the entire ICBs

It is difficult to evaluate how phosphorylation can, if at all, determine the localization of syndecan-4 to the midbody region. Because of the diverse stainings of SDC4 in the midbody region the distribution of the phosphorylated and non-phosphorylated forms was studied by using green fluorescent protein (GFP)-tagged mutants. The plausible C-terminal fusion of GFP did not provide adequate results in our tests contrary to the published data [28], thus GFP was inserted into the juxtamembrane region of the extracellular domain to avoid the interference with the natural interacting partners of the cytoplasmic domain (Fig. 3a). In the GFP-tagged SDC4 Ser179 was replaced by Glu (Ser179Glu), which is considered to mimic the phospho-serine in biological systems, or by Ala (Ser179Ala) as phosphorylation resistant form. The constructs were transfected into MCF-7 cells and stably expressing lines were studied. The distribution of wt-SDC4-GFP (Fig. 3b) was identical to that of non-tagged wt-SDC4 (Fig. 1b, c). GFP alone showed a diffuse distribution (Fig. 3b).

Cells expressing the SDC4-GFP chimeras had the same adhesion properties and reacted identically in biochemical tests to those expressing the non-tagged SDC4 (to be published elsewhere). No difference was found between cytochemical markers of the cells expressing GFP-tagged or non-tagged SDC4 variants in the experiments performed with several independent expressing cell lines (Figs. 1, 2, 3).

The expression level of the different SDC4 constructs (wt-SDC4-GFP, Ser179Ala, or Ser179Glu) was similar in immunoblot (Fig. 4e, see later). The proliferation rate of the cell lines was not altered compared to that of MCF-7 (Suppl. Fig. 2).

The wt-SDC4-GFP chimera localized in the intercellular bridges and accumulated at the midbodies (Fig. 3c1). The distribution of the Ser179Ala SDC4 showed massive plasma membrane enrichment in the interphase cells, but it could not be detected with mitotic spindles and was absent from the entire ICB (Fig. 3c2). Its detection at midbodies failed even if the signal was amplified with anti-GFP immunostaining. On the contrary, the Ser179Glu mutant was concentrated in the ICBs, enriched at the midbodies in mitotic cells (Fig. 3c3) and it was hardly observed in the plasma membrane of interphase cells.

Together, wt-SDC4-GFP and the phosphomimetic Ser179Glu chimera were enriched at midbodies corroborating the result of the staining with anti-SDC4-ecto antibody. We assumed that the short antigen determinant recognized by the anti-P-SDC4 antibody must be present at the midbody but it is not accessible because of the high protein density. It occurs frequently that antibodies raised against different epitopes react differently with the antigens depending on the accessibility of the epitopes [29].

Shedding of syndecan-4 occurs at G2/M phases

To confirm the specificity of the antibodies, cell lysate of wt-SDC4 line was subjected to immunoblot analysis using the anti-SDC4-ecto, anti-SDC4-endo or anti-P-SDC4 antisera (Fig. 4a, b). Two strong signals were detected at 45 and 22 kDa electrophoretic mobility both by anti-SDC4-ecto and anti-SDC4-endo antibodies, corresponding to the syndecan-4 dimer and monomer, respectively. However, two additional bands at 13 and 6 kDa were visualized by

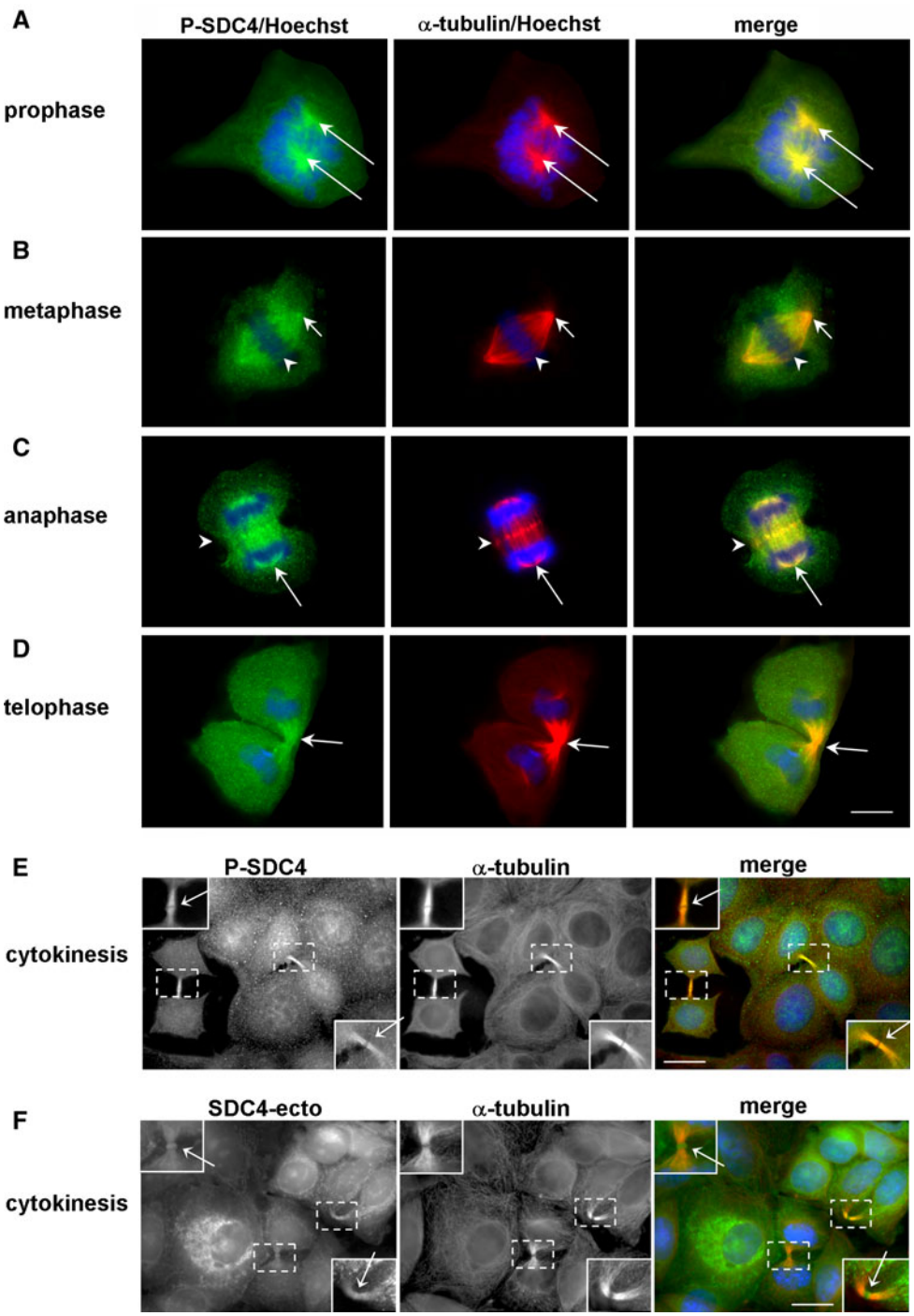

Fig. 2 Phospho-syndecan-4 associates with the mitotic spindle. MCF-7 cells expressing wt-SDC4 were immunostained for phospho-SDC4 with anti-P-SDC4 (sc-22252-R, *green*), α-tubulin (*red*) and nuclei (Hoechst, *blue*). The phospho-SDC4 was co-localized with the MTOCs from the early prophase until anaphase (**a**–**c**; *arrows*). As mitosis progressed, phospho-SDC4 was distributed along the mitotic spindle and accumulated in the spindle midzone (**b**, **c**; *arrowheads*), later it was enriched in the cleavage furrow (**d**; *arrows*) and subsequently in the ICB (**e**; *arrows*). Note that the midbody was not immunoreactive for anti-P-SDC4 (**e**). MCF-7 cells expressing wt-SDC4 were immunostained with anti-SDC4-ecto (*green*), α-tubulin (*red*) antibodies, and Hoechst (*blue*) (**f**). Full-length syndecan-4 was enriched at the midbodies (*arrows*). The *insets* show magnification of the areas framed by *dashed squares*. *Scale bars* represent 20 μm

the anti-SDC4-endo antiserum and they were considered as SDC4 shed remnants (Fig. 4a). Since all the bands were also detected by the anti-P-SDC4 antisera and could be diminished upon the addition of increasing concentration of the immunogenic phospho-peptide the immunoreaction was specific (Fig. 4b). The pattern altogether confirmed that the shed remnants are, at least partly, phosphorylated.

We assumed that the distinct immunostaining pattern of the anti-SDC4-ecto and anti-P-SDC4 antisera (Fig. 1) could be a consequence of shedding, which can promote cell detachment and rounding-up during mitosis via breaking up the interactions of the matrix and the extracellular domain of syndecan-4. To test this hypothesis, the wt-SDC4-expressing MCF-7 line was synchronized by the addition of 1.5 mM hydroxyurea, which blocks the cell cycle in G1/S transition. Releasing the cells from the block the cell cycle progressed and it was followed by flow cytometry. At least 50% of the cells doubled their DNA

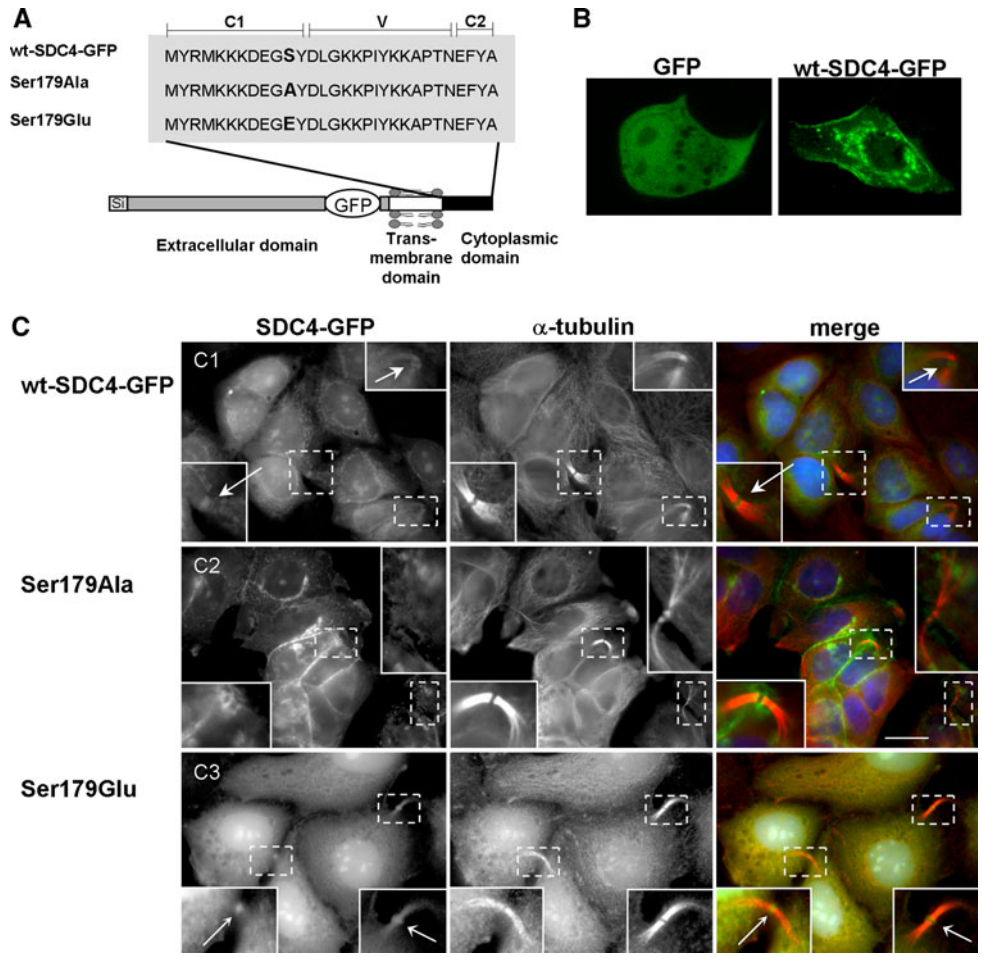

Fig. 3 Only the Ser179Glu SDC4 accumulates in the ICBs. **a** Schematic representation of full-length, GFP-tagged syndecan-4 variants. The conserved C1, C2 and the variable V regions of the cytoplasmic domain are marked. Ala or Glu mutations were introduced into the position of 179 as indicated. GFP was inserted into the juxtamembrane region of the extracellular domain of syndecan-4 (wt-SDC4-GFP); the Ser179Ala and Ser179Glu mutants were generated from the wt-SDC4-GFP. **b** Cellular distribution of GFP-tagged SDC4 (wt-SDC4-GFP) and GFP alone. **c** MCF-7 cells expressing wt-SDC4-GFP, Ser179Ala or Ser179Glu SDC4 (*green*) were immunostained with α-tubulin antibody (*red*) and Hoechst (*blue*). The GFP-tagged wild-type syndecan-4 was detected in the ICBs and an accumulation could be observed at the midbodies, indicated by *arrows* (**c1**). The Ser179Ala SDC4 was missing from the entire ICB regions (**c2**), while Ser179Glu SDC4 was observed in ICBs and enriched at the midbodies (**c3**) pointed by *arrows*. *Insets* show a magnification of the areas indicated by *dashed squares*. *Scale bar* represents 20 μm

content by 3 h after removal of hydroxyurea. At 6 h, the populations of 2N cells started increasing, meaning that the given ratio of the cells had already accomplished cytokinesis. By 18 h, only a small fraction of 4N cells was observed (Fig. 4c).

The intact SDC4 and the shed remnants were monitored by immunoblotting during the cell cycle using anti-SDC4-endo and anti-P-SDC4 antibodies. An equal number of cells were lysed and subjected to PAGE. The level of SDC4 alternated during the studied period as the cell cycle progressed. In 3 h, the level of full length was reduced then gradually increased until 15 h, then it decreased again to the level of the control (Fig. 4d1). However, the phosphorylation of SDC4 increased markedly following the release of the cell cycle block reaching the maximum at 6 h and decreasing to the basic level after 18 h (Fig. 4d2). The pattern of the shed remnant and the phospho-shed remnant was corresponding to that of the phosphorylated full-length SDC4 reaching the most intense signal at 6 h after the removal of hydroxyurea (Fig. 4d1, d2). This means that the phospho-syndecan-4 underwent the process of shedding instead of the shed remnants being phosphorylated.

Only the phospho-Ser179 syndecan-4 can be shed during the cell cycle

To confirm that the phospho-SDC4 was subjected to shedding, the lysates of wt-SDC4-GFP-, Ser179Ala-, and Ser179Glu SDC4-expressing cells were probed with anti-

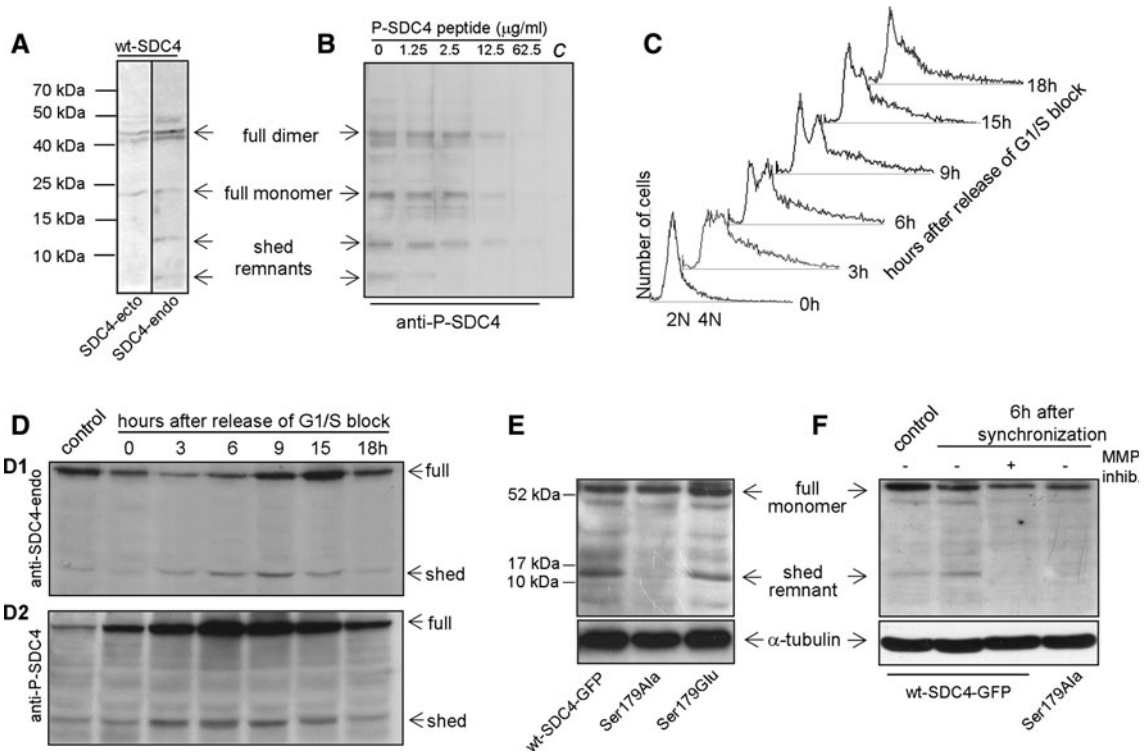

Fig. 4 The phosphorylation and shedding of SDC4 increased during the G2/M phase. **a** The lysates of wt-SDC4 line were subjected to SDS-PAGE, blotted and probed with anti-SDC4-ecto or anti-SDC4-endo antibodies, respectively. The full-length SDC4 dimer and monomer were detected with both antibodies at 45 and 22 kDa, respectively. The anti- SDC4-endo antibody stained an extra band at 13 kDa and a fainter one at 6 kDa corresponding to the shed syndecan-4 remnants. **b** In peptide competition assay, the aliquots of the wt-SDC4 lysate were subjected to SDS-PAGE, followed by immunoprobing with 1:1,000 diluted anti-P-SDC4, which was supplemented with increasing amounts of phospho-syndecan-4 peptide. The last lane as negative control, marked *C*, was incubated only with the secondary reagent. **c** The DNA content of the wt-SDC4 expressing cells was analyzed by flow-cytometry after release from G1/S block. Exponentially growing wt-SDC4 expressing MCF-7 cells were synchronized with 1.5 mM hydroxyurea for 16 h. Cells were harvested at 0, 3, 6, 9, 15, 18 h after removal of hydroxyurea to allow the progression along the cell cycle. **d** Cells were harvested at the indicated time points as in **c**, and equal number of cells were lysed and subjected to SDS-PAGE followed by immunoblotting with anti-SDC4-endo (**d1**) or anti-P-SDC4 (**d2**) antibodies. The level of the full length SDC4 was changed following release of G1/S block as the cell cycle progressed. The level of phosphorylated and the shed form was changed parallel: both increased from 3 h, reaching the maximum at 6 h and returned to the base line at 18 h. The control lane contains the lysates of asynchronously grown wt-SDC4 cells. **e** The lysates of asynchronous cell populations expressing wt-SDC4-GFP, Ser179Ala and Ser179Glu were subjected to SDS-PAGE and blotted with anti-SDC4-endo antibody. Anti-α-tubulin antiserum was used as a loading control. The expression levels of the full-length monomers were similar; however, the anti-SDC4-endo antibody visualized a 13 kDa band representing the shed remnant, which was missing in the lysates of Ser179Ala mutant cells. **f** MCF-7 cells expressing wt-SDC4-GFP and Ser179Ala SDC4 were synchronized as stated before. Upon removal of the hydroxyurea, the medium was complemented with a broad-spectrum MMP inhibitor GM6001, marked in the panel (+), and 6 h later the samples were lysed and subjected to SDS-PAGE followed by immunoblotting with anti-SDC4-endo antibody. The asynchronous control (*lane 1*) and the synchronized wt-SDC4-GFP (*lane 2*) samples contained the 13 kDa band corresponding to the shed remnant. This band was missing from the samples of the protease inhibitor treated (*lane 3*) and the Ser179Ala expressing cell line (*lane 4*). Anti-α-tubulin antiserum was used as a loading control

SDC4-endo antibody. In the samples of wt-SDC4-GFP and Ser179Glu, an extra band was observed corresponding to the shed remnant form that was missing in the Ser179Ala expressing cells, although the expression levels of the full-length monomers were similar (Fig. 4e). In parallel experiments, the wt-SDC4-GFP and Ser179Ala cell lines were synchronized and the shed form was tested. Six hours following the release of the cell cycle block, the band corresponding to the shed forms was seen in the wt-SDC4-GFP sample, however, it was missing in the sample of Ser179Ala expressing cell line (Fig. 4f). This confirmed that only the phospho-Ser179 form could undergo the process of ectodomain shedding. To prove the specificity of the anti-SDC4-endo antibody, the lysates of wt-SDC4-GFP-expressing cells were blotted and immunostained with anti-GFP and anti-SDC4-endo antibodies, respectively (Suppl. Fig. 1b).

The ectodomain of syndecans can be cleaved mostly by matrix metalloproteinases (MMPs) [18–20, 30]. To verify that the 13 kDa band was a result of proteolysis, a broad spectrum metalloproteinase inhibitor was applied to the cells expressing wt-SDC4-GFP. Samples were collected

6 h following the release of G1/S block, when the level of shed remnant was at maximum (Fig. 4d), and analyzed by immunoblotting. Administration of the MMP inhibitor diminished the 13 kDa band, whereas the similarly synchronized sample of wt-SDC4-GFP contained it (Fig. 4f), indicating that this band was the result of proteolytic cleavage.

Midbody localization of syndecan-4 requires proper membrane insertion

We showed earlier that the full-length SDC4 enriched at midbodies. It is not obvious whether an inside or outside interaction is necessary to move SDC4 to the midbody. To answer this, truncated forms of SDC4 were generated from the phosphomimicking Ser179Glu SDC4 with deletion of a part of the ectodomain (signal-DEGE). In order to study the behavior of the cytosolic and the membrane-targeted proteins, we generated a signal-deleted version from signal-DEGE, named DEGE (Fig. 5a).

The expression levels and electrophoretic mobilities of the DEGE and the signal-DEGE proteins were matched in immunoblot indicating equal expression and proper removal of the signal peptide upon secretion. The total cell lysates of both cell lines were separated to cytoplasmic and membrane fractions by ultracentrifugation (Fig. 5b). Expression of the signal-deleted DEGE construct resulted in cytosolic protein, whereas the protein translated from signal-DEGE construct was targeted mostly to the membrane fraction (Fig. 5b).

The two proteins localized differently in vivo. The DEGE was dispersed in the cytoplasm and enriched in the ICBs of mitotic cells without significant accumulation at the midbodies (Fig. 5c). On the contrary, signal-DEGE was observed in the ICBs and enriched at the midbodies (Fig. 5c) similarly to the full-length Ser179Glu SDC4.

Taken together, the correct midbody enrichment of SDC4 needed membrane insertion of the transmembrane domain in addition to the phosphorylation of the cytoplasmic domain, but the ectodomain was dispensable. Similar to the phospho-SDC4, the phosphomimicking SDC4 could escape from the membrane into the cytoplasm.

Expression of the Ser179Ala syndecan-4 can lead to multinucleated giant cells

So far, the distribution of the phospho-mimicking and phospho-resistant forms was examined. However, the

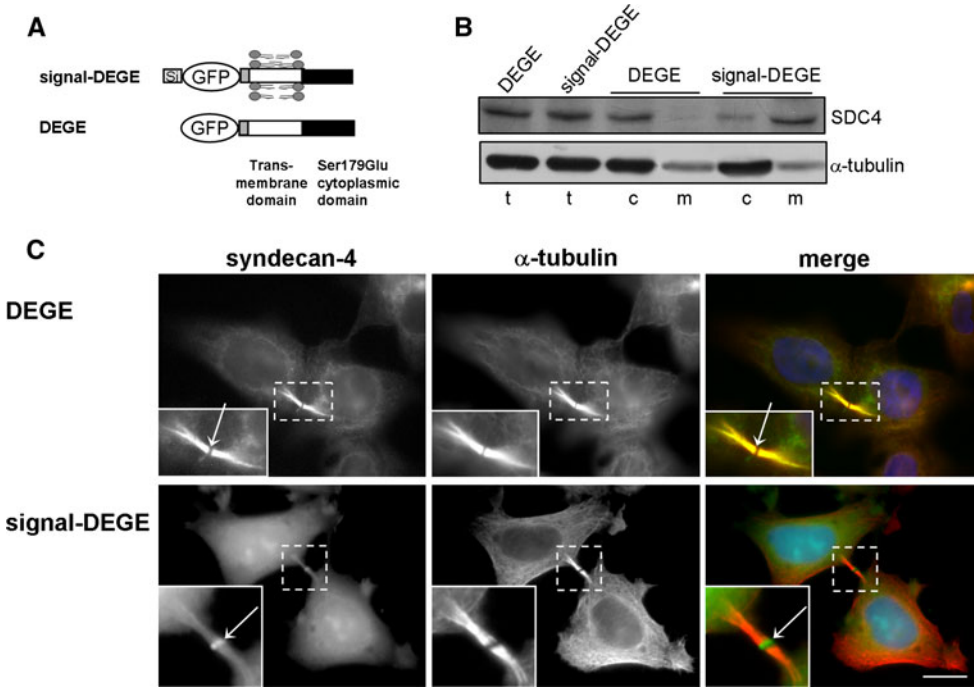

Fig. 5 Membrane insertion is needed to midbody localization. **a** Schematic figure represents the shed syndecan-4 variants. Deletion of a part of the ectodomain of Ser179Glu resulted in signal-DEGE, and then the signal was deleted from signal-DEGE named DEGE. **b** Lysates of cells expressing DEGE and signal-DEGE were fractionated. The total (*t*), cytosol (*c*), and membrane (*m*) fractions were resolved by SDS-PAGE and subjected to immunoblotting with anti-GFP antibody; anti-α-tubulin antiserum was used as a loading control. A representative sample from three independent experiments is shown. **c** Microtubules of DEGE and signal-DEGE expressing cell lines are visualized by anti-α-tubulin (*red*). The DEGE (*green*) distributed homogenously in the ICB, but was missing from midbody (*arrow*), whereas signal-DEGE (*green*) accumulated at the midbodies (*arrow*). *Scale bar* 10 μm

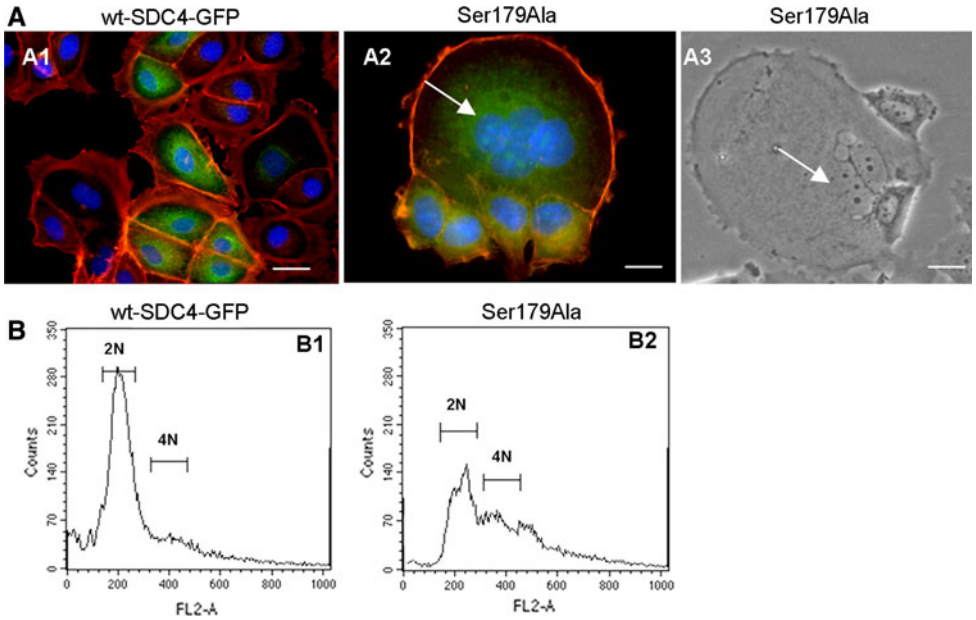

Fig. 6 The mutations of syndecan-4 Ser179 lead to phenotypic alterations. **a** Actin cytoskeleton of MCF-7 cells expressing wt-SDC4-GFP (**a1**) or Ser179Ala syndecan-4 (**a2**) was visualized by TRITC-phalloidin (*red*). In the wt-syndecan-4-expressing cells (**a1**) actin belts separated the abutting cells from each other. Ser179Ala cells (**a2**) were frequently detected as multinucleated cells encircled by a thick actin ring. Mononuclear cells encircled by cortical actin rings were attached to the giant cell. Phase-contrast micrograph of a multinucleated, giant cell is shown in **a3**. *Arrows* point at the nuclei of the multinucleated cells in the Ser179Ala population (**a2**, **a3**). The nuclear staining is *blue*; the *scale bars* represent 20 μm. **b** FACS analysis of wt-SDC4-GFP and Ser179Ala lines. The cells were fixed and permeabilized prior to propidium iodide staining of nuclei and analyzed by flow cytometry. Wt-SDC4-GFP cells presented a normal profile of proliferating cell population with a dominant 2N and a minor 4N peak (**b1**). However, the profile was changed in the Ser179Ala expressing cells (**b2**). The relative amount of 2N cells was decreased, the 4N was increased, and the baseline was elevated. These results are representative of at least three independent experiments

different forms induced altered phenotypes. The wt-SDC4-GFP-expressing cells showed a typical epithelial character, closely packed cells each encircled by an actin belt, which was visualized by phalloidin (Fig. 6a1). However, in the Ser179Ala line, frequently giant multinucleated cells were observed in the epithelial cell clusters. The ratio of the multinucleated cells was characterized from the transfection as starting point and monitored weekly. The ratio of the multinucleated cells in the Ser179Ala line was increasing until the first passage (4 weeks) to 5% then the normally dividing cells diluted gradually the multinucleated cells to a steady state frequency of $1 \pm 0.05\%$ ($n = 10^5$). The size of the syncytia could be as large as several dozen cells (Fig. 6a2, a3). There were no multinucleated cells developed in the original MCF-7 line during the studied period.

To validate the multinucleated phenotype asynchronously growing cells were fixed, stained with propidium iodide, and analyzed by flow cytometry. Control wt-SDC4-GFP expressing cells exhibited a typical profile of proliferating cell population ($n = 55{,}000$) with a dominant peak of 2N DNA content (56%), and a smaller peak with 4N DNA content (8%), which represented the G2/M phase cells (Fig. 6b1). The Ser179Ala cells showed altered profile; the relative number of 2N cells representing the G1 phase decreased to 34%, the 4N cells increased to 18% (Fig. 6b2). Overall, the base line was shifted in the >4N region indicating the increased content of DNA of the cells.

The ratio of multikaryons slowly increased in the Ser179Glu expressing line, too. There were no multinucleated cells observed until two to three passages, however, the number of multikaryons increased continuously to 5% ($n = 55{,}000$) in 6 months, most probably because of the incomplete cytokinesis. In this case, the polynucleation was not connected to the enlarged cell size. There were no multinucleated cells detected in the original MCF-7 line during 6 months propagation.

Time-laps analysis of the mitotic phase reveals the difference during the cytokinesis of the different cell lines

Different asynchronous proliferating cell cultures were monitored by phase-contrast time-lapse photography. Selected frames are shown in Fig. 7a. The cells of non-transfected MCF-7 (Fig. 7a1, Suppl. Video 1), and Ser179Ala (Fig. 7a2, Suppl. Video 2) expressing lines

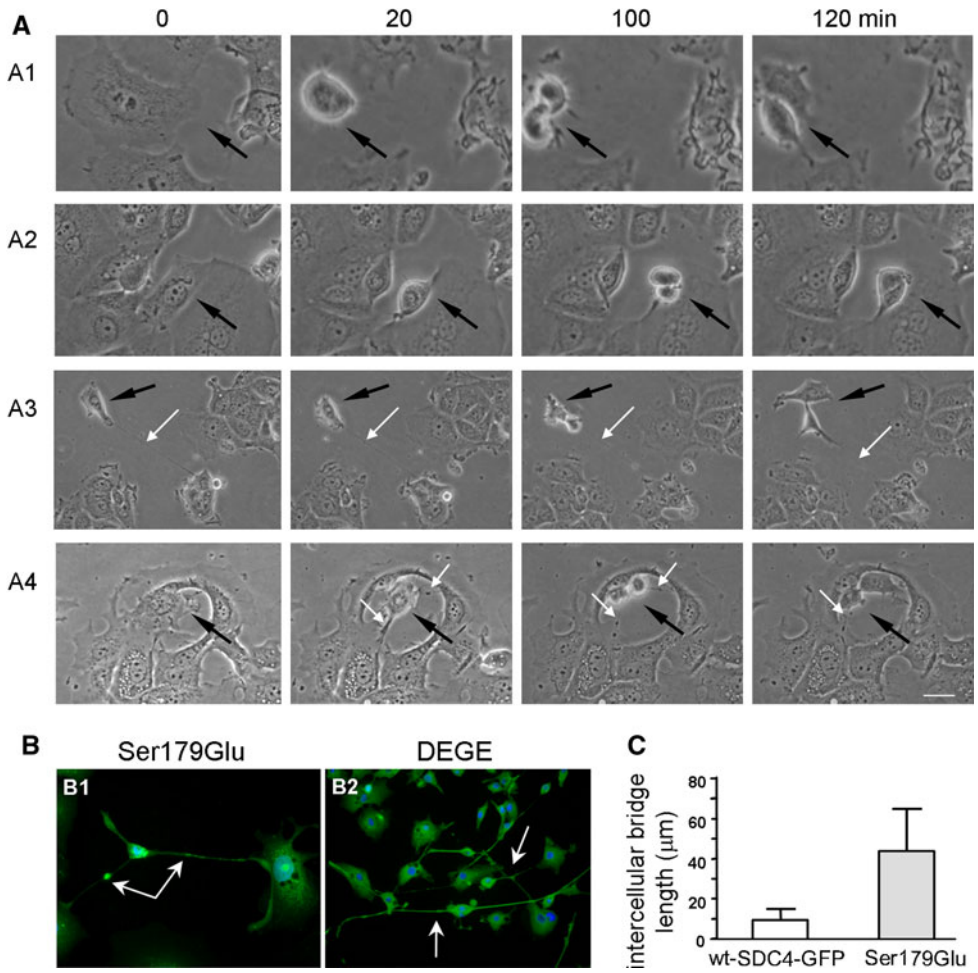

Fig. 7 The Ser179Glu mutation of syndecan-4 causes failure in cytokinesis. **a** Different asynchronous proliferating cell cultures were monitored by phase-contrast time-lapse photography. Selected frames are shown, in which the proliferating cells are pointed by *black arrows*. The cells of MCF-7 (**a1**) and Ser179Ala expressing lines (**a2**) separate from the neighboring cells during rounding-up, while the cells expressing Ser179Glu SDC4 (**a3**) or the DEGE (**a4**) construct remain connected to the ex-mother cells by permanent cytoplasmic bridges shown by *white arrows*. *Bar* 25 μm. **b** Expression of Ser179Glu (**b1**) or DEGE (**b2**) (*green*) resulted in elongated, axon-like ICBs. Ser179Glu or DEGE constructs (*green*) were enriched in the cytoplasm and at the midbodies. The failure of abscission resulted in long thread, which connected several cells together. *White arrows* show the midbodies (*scale bar* 20 μm). **c** The average length of ICBs in cells expressing wt-SDC4-GFP or Ser179Glu are represented ($n = 100$). The length of the ICBs of Ser179Glu (45.4 ± 18.28 μm) was extended 4.5-fold compared to that of the wt-SDC4-GFP (9.8 ± 4.23 μm)

rounded-up at the beginning of the mitosis breaking all of the attachments to their neighbors resulting in completely separated cells. In the meanwhile, the cells expressing any Ser179Glu mutants Ser179Glu (Fig. 7a3, Suppl. Video 3), or DEGE (Fig. 7a4, Suppl. Video 4) remained connected to the ex-mother cells by permanent cytoplasmic bridges. These bridges were not cleaved at the end of the cytokinesis. They remained permanent and appeared later as elongated ICBs (Fig. 7b). The average length of the ICBs varied between 8.5 and 14 μm in nt-MCF-7, wt-SDC4-GFP and Ser179Ala expressing cells, however, in the Ser179Glu line that value increased to 45.4 ± 18.28 μm ($n = 100$) (Fig. 7c), which sometimes exceeded 200 μm. The expression of phosphomimetic mutants frequently developed network of cells linking 5 or even more cells together by long, thin plasma threads (Fig. 7b).

Discussion

Before and during mitosis, normally adherent cells round up and reorganize their adhesive interactions with the extracellular matrix; executing cytokinesis the cells start reattaching and spreading again [2]. Syndecan-4 influences the connection between the cells and the surrounding ECM [9, 14]. The cleavage of the extracellular domain of SDC4 is a natural process [18], which in turn can promote cell detachment and round up. As a consequence of shedding,

the ectodomains are regularly released into the surrounding milieu [18], however, the fate of the shed syndecan-4 remnants was mostly unknown [20].

Here we reported that phosphorylation of the cytoplasmic domain and cleavage of the extracellular domain of syndecan-4 changed periodically during the cell cycle, reaching the maximum at G2/M phases. Furthermore, only the phospho-SDC4 could undergo cell cycle-induced ectodomain shedding. At the same time, a part of the phospho-SDC4 could escape from the membrane to the cytosol, distributed along the mitotic spindle and consequently accumulated in the intercellular bridge formed at the end of mitosis. However, to the midbody localization of SDC4, the correct membrane insertion was necessary. Depending on its phosphorylation status, SDC4 promoted the cytokinesis: expression of the phosphomimicking form aborted the final step of cytokinesis, while phospho-resistant mutant of SDC4 resulted in multinucleated cells. Therefore the shedding has a dual effect: on one hand it helps rounding-up with breaking the cell adhesions, and on the other hand, the phosphorylated shed remnants influenced the progression of cytokinesis. Further, the cell-cycle regulated shedding can explain the long-time-known phenomenon of regular shedding in tissue culture, which was characterized hitherto in asynchronously growing, cultured cell populations.

Several factors, chemokines and other stimulators, can induce the process of shedding, however, the exact nature of shedding is still unknown [18, 30–32]. Recently an inside-out signaling mechanism was revealed, which supposed to regulate the ectodomain shedding by the interaction between Rab5 (a small GTPase) and the cytoplasmic domain of syndecan-1 [31]. Here we suggested that the phosphorylation of the cytoplasmic domain regulated the ectodomain cleavage. Whether this mechanism is connected to the Rab5 mechanism needs further investigation.

Prerequisite of the mitotic spindle association is the cytoplasmic distribution of the interacting proteins, therefore the enrichment of syndecan-4 or its shed remnants along the spindles assumes proteins released from the membrane. Since the protein detected along the spindle was phosphorylated and there was no sign that non-phosphorylated protein would associate to spindle, we surmise that only the phosphorylated proteins could be guided to the midbodies and escape from the membrane.

The elevated rate of the endoreduplication can be caused by default of phosphorylation. The expression of the Ser179Ala protein could result in stronger cell anchorage, that is, cell–cell, and cell–matrix adhesions could not be broken at the beginning of mitosis, due to the fault of the shedding process of the phospho-defective Ser179Ala mutation, further, the non-phosphorylated version could not escape from the membrane.

The association of SDC4 to the spindle assumes interaction with tubulin [22]. Although the syndecan–tubulin interaction was already shown [33], this could not be direct interaction, because SDC4 was detected only with the mitotic spindles and not with the microtubules in interphase cells. Therefore, the binding of syndecan-4 to the microtubules should be mediated through spindle-associated protein(s).

The accumulation of syndecan-4 in the ICBs and at the midbodies requires phosphorylation of syndecan-4, since the phospho-resistant Ser179Ala form was missing from the whole midbody region and was not observed along the mitotic spindle. However, the accumulation of syndecan-4 in the ICBs and/or at the midbodies should be independent processes, since the midbody enrichment needed the correct membrane localization besides phosphorylation, and the shed remnants were enriched only in the ICBs alongside the spindles leaving the midbodies empty. Therefore, the presence of the spindle-associated shed remnants in the ICBs is most probably an inevitable consequence of the arrayed mitotic spindles. The full syndecan-4, however, should be recruited to the midbodies in an alternative way. Wt-SDC4 was distributed at the ICBs in asymmetrically arrayed vesicles (Figs. 2f1, 3c1) rather than a homogenous dispersion along the spindles that was seen in the cases of the shed remnants. This phenomenon suggests that full-length SDC4 was delivered in vacuoles to the midbodies.

The extended length of ICBs of Ser179Glu mutant cells is a consequence of the failure of abscission. The length of the ICBs might depend on the position of the re-attaching cells showed by time-laps photos; the daughter cells placed farther from each other yet remained connected by long, thin plasma bridge (Fig. 7a3, a4 and Suppl. Videos 3, 4). CHO1 a member of the MKLP family is a kinesin-like motor protein, which was found essential for completion of cytokinesis in mammalian cells; its mutation resulted in similar phenotype: extended, thin ICBs [34].

Several transmembrane proteins have already been observed at the midbody [4, 29]. For example the tight junction proteins: claudin-1 and occludin were detected at the midbodies, whereas the also tight junction, but cytoplasmic ZO proteins were missing [29]. This means, that there should be a mechanism that orients transmembrane proteins to the midbody. Therefore, the enrichment of transmembrane syndecan-4 at the midbodies is the consequence of a guided event.

The mechanism of the abscission involves membrane fusion events; otherwise, the plasma membranes of the newly generated daughter cells would be ruptured [3, 35, 36]. Dynamin, a large GTPase protein that controls a variety of vesicular budding events, was found to associate with the spindle midzone and is required for cytokinesis [37]. The dynamin is an interacting partner of syndecan-4

binding the conservative C1 domain of syndecan-4 [38] that comprises the Ser179, however, the consequence of this interaction for the membrane dynamics has not been known. Rab5 is one of the Rab small GTPases that regulates a variety of intracellular trafficking such as membrane trafficking into and between early endosomes and vesicle transport along microtubules [39]. Rab5-GDP was reported that it interacted with the conserved segment of the cytoplasmic domain of syndecans [31]. Therefore, SDC4 can interact with Rab5; herewith it could be the link between the vesicle transports along the microtubule and motor proteins.

The importance of Rho-family small GTPases in the cytokinesis has been known for a long time but their exact role has not yet been completely elucidated. The guanine-nucleotide exchange factors (GEFs) of Rho-family ECT2 and TD-60, or Rho-GTPase-activating proteins (Rho-GAPs) MgcRacGAP, and p190RhoGAP were found implicated in the regulation of cytokinesis [5, 40–43]. Syndecan-4 could influence p190RhoGAP activity [44] and also determine the Rac activity [45, 46] according to our studies in a phosphorylation-dependent manner (unpublished data), which in turn can lead to failure of abscission. Malfunction of the Rho-ROCK kinase pathway resulted in similarly extended ICBs formed between the unseparated daughter cells in T24 cell line [47]. The perturbation of the phosphorylation of MgcRacGAP, which in turn can determine its Rho/Rac GAP activity, arrested cytokinesis at a late stage and induced polyploidy [48]. Since SDC4 is involved in the regulation of Rho-Rac activity thus we surmise that it can promote the completion of cytokinesis.

The observed anomalies in the cytokinesis clearly indicated the functional role of the phosphorylation and shedding of syndecan-4 and suggested that the spatio-temporal regulation of the nonphosphorylated and phosphorylated syndecan-4 must be important for the proper execution of the mitosis. Syndecan-4 can be a link for transmitting signals from the ECM to the cell that regulate not only cell adhesion but cell proliferation, as well.

Acknowledgments The authors are indebted to Dr. Ibolya Kiss to share the cell culture facilities and Edit Kotogany for the technical assistance in the FACS experiments. A.K.-P. received a fellowship from the Gedeon Richter Centenary Foundation. This work was supported by grants KFP1-00024/2005 to L.S; NKTH-OM-00087/2007 and OTKA T049608 to F.D.; OTKA NK72595 to J.T.

References

1. Glotzer M (2001) Animal cell cytokinesis. Annu Rev Cell Dev Biol 17:351–386
2. Piel M, Nordberg J, Euteneuer U, Bornens M (2001) Centrosome-dependent exit of cytokinesis in animal cells. Science 91:1550–1553
3. Barr FA, Gruneberg U (2007) Cytokinesis: placing and making the final cut. Cell 131:847–860
4. Skop AR, Liu H, Yates J III, Meyer BJ, Heald R (2004) Dissection of the mammalian midbody proteome reveals conserved cytokinesis mechanisms. Science 305:61–66
5. Glotzer M (2005) The molecular requirements for cytokinesis. Science 307:1735–1739
6. Greenbaum MP, Yan W, Wu MH, Lin YN, Agno JE, Sharma M, Braun RE, Rajkovic A, Matzuk MM (2006) TEX14 is essential for ICBs and fertility in male mice. Proc Natl Acad Sci USA 103:4982–4987
7. Woods A, Couchman JR (2001) Syndecan-4, focal adhesion function. Curr Opin Cell Biol 13:578–583
8. Mostafavi-Pour Z, Askari JA, Parkinson SJ, Parker PJ, Ng TT, Humphries MJ (2003) Integrin-specific signaling pathways controlling focal adhesion formation and cell migration. J Cell Biol 161:155–167
9. Morgan MR, Humphries MJ, Bass MD (2007) Synergistic control of cell adhesion by integrins and syndecans. Nat Rev Mol Cell Biol 8:957–969
10. Bernfield M, Kokenyesi R, Kato M, Hinkes MT, Spring J, Gallo RL, Lose EJ (1992) Biology of the syndecans: a family of transmembrane heparan sulfate proteoglycans. Annu Rev Cell Biol 8:365–393
11. Kokenyesi R, Bernfield M (1994) Core protein structure and sequence determine the site and presence of heparan sulfate and chondroitin sulfate on syndecan-1. J Biol Chem 269:12304–12309
12. Langford JK, Stanley MJ, Cao D, Sanderson RD (1998) Multiple heparan sulfate chains are required for optimal syndecan-1 function. J Biol Chem 273:29965–29971
13. Carey DJ (1997) Syndecans: multifunctional cell-surface co-receptors. Biochem J 327:1–16
14. Rapraeger AC, Ott VL (1998) Molecular interactions of the syndecan core proteins. Curr Opin Cell Biol 10:620–628
15. Couchman JR, Vogt S, Lim ST, Lim Y, Oh ES, Prestwich GD, Theibert A, Lee W, Woods A (2002) Regulation of inositol phospholipid binding and signaling through syndecan-4. J Biol Chem 277:49296–49303
16. Lim ST, Longley RL, Couchman JR, Woods A (2003) Direct binding of syndecan-4 cytoplasmic domain to the catalytic domain of protein kinase C alpha (PKC alpha) increases focal adhesion localization of PKC alpha. J Biol Chem 278:13795–13802
17. Koo BK, Jung YS, Shin J, Han I, Mortier E, Zimmermann P, Whiteford JR, Couchman JR, Oh ES, Lee W (2006) Structural basis of syndecan-4 phosphorylation as a molecular switch to regulate signaling. J Mol Biol 355:651–663
18. Fitzgerald ML, Wang Z, Park PW, Murphy G, Bernfield M (2000) Shedding of syndecan-1 and -4 ectodomains is regulated by multiple signaling pathways and mediated by a TIMP-3-sensitive metalloproteinase. J Cell Biol 148:811–824
19. Li Q, Park PW, Wilson CL, Parks WC (2002) Matrilysin shedding of syndecan-1 regulates chemokine mobilization and transepithelial efflux of neutrophils in acute lung injury. Cell 111:635–646
20. Wang Z, Götte M, Bernfield M, Reizes O (2005) Constitutive and accelerated shedding of murine syndecan-1 is mediated by cleavage of its core protein at a specific juxtamembrane site. Biochemistry 44:12355–12361
21. Yaffe D, Saxel O (1977) Serial passaging and differentiation of myogenic cells isolated from dystrophic mouse muscle. Nature 270:725–727

22. Brockstedt U, Dobra K, Nurminen M, Hjerpe A (2002) Immunoreactivity to cell surface syndecans in cytoplasm and nucleus: tubulin-dependent rearrangements. Exp Cell Res 274:235–245
23. Echtermeyer F, Baciu PC, Saoncella S, Ge Y, Goetinck PF (1999) Syndecan-4 core protein is sufficient for the assembly of focal adhesions and actin stress fibers. J Cell Sci 112:3433–3441
24. Simons M, Horowitz A (2001) Syndecan-4-mediated signalling. Cell Signal 13:855–862
25. Horowitz A, Tkachenko E, Simons M (2002) Fibroblast growth factor-specific modulation of cellular response by syndecan-4. J Cell Biol 157:715–725
26. VanWinkle WB, Snuggs MB, De Hostos EL, Buja LM, Woods A, Couchman JR (2002) Localization of the transmembrane proteoglycan syndecan-4 and its regulatory kinases in costameres of rat cardiomyocytes: a deconvolution microscopic study. Anat Rec 268:38–46
27. Horowitz A, Simons M (1998) Regulation of syndecan-4 phosphorylation in vivo. J Biol Chem 273:10914–10918
28. Paris S, Burlacu A, Durocher Y (2008) Opposing roles of syndecan-1 and syndecan-2 in polyethyleneimine-mediated gene delivery. J Biol Chem 283:7697–7704
29. Kojima T, Kokai Y, Chiba H, Osanai M, Kuwahara K, Mori M, Mochizuki Y, Sawada N (2001) Occludin and claudin-1 concentrate in the midbody of immortalized mouse hepatocytes during cell division. J Histochem Cytochem 49:333–340
30. Schmidt A, Echtermeyer F, Alozie A, Brands K, Buddecke E (2005) Plasmin- and thrombin-accelerated shedding of syndecan-4 ectodomain generates cleavage sites at Lys(114)-Arg(115) and Lys(129)-Val(130) bonds. J Biol Chem 280:34441–34446
31. Hayashida K, Stahl PD, Park PW (2008) Syndecan-1 ectodomain shedding is regulated by the small GTPase Rab5. J Biol Chem 283:35435–35444
32. Bass MD, Morgan MR, Humphries MJ (2009) Syndecans shed their reputation as inert molecules. Sci Signal 64:pe18
33. Zimmermann P, David G (1999) The syndecans, tuners of transmembrane signaling. FASEB J 13:S91–S100
34. Matuliene J, Kuriyama R (2004) Role of the midbody matrix in cytokinesis: RNAi and genetic rescue analysis of the mammalian motor protein CHO1. Mol Biol Cell 15:3083–3094
35. Low SH, Li X, Miura M, Kudo N, Quiñones B, Weimbs T (2003) Syntaxin 2 and endobrevin are required for the terminal step of cytokinesis in mammalian cells. Dev Cell 4:753–759
36. Glotzer M (2003) Cytokinesis: progress on all fronts. Curr Opin Cell Biol 15:684–690
37. Thompson HM, Skop AR, Euteneuer U, Meyer BJ, McNiven MA (2002) The large GTPase dynamin associates with the spindle midzone and is required for cytokinesis. Curr Biol 12:2111–2117
38. Yoo J, Jeong MJ, Cho HJ, Oh ES, Han MY (2005) Dynamin II interacts with syndecan-4, a regulator of focal adhesion and stress-fiber formation. Biochem Biophys Res Commun 328:424–431
39. Zerial M, McBride H (2001) Rab proteins as membrane organizers. Nat Rev Mol Cell Biol 2:107–117
40. Piekny A, Werner M, Glotzer M (2005) Cytokinesis: welcome to the Rho zone. Trends Cell Biol 15:651–658
41. Su L, Agati JM, Parsons SJ (2003) p190RhoGAP is cell cycle regulated and affects cytokinesis. J Cell Biol 163:571–582
42. Mollinari C, Reynaud C, Martineau-Thuillier S, Monier S, Kieffer S, Garin J, Andreassen PR, Boulet A, Goud B, Kleman JP, Margolis RL (2003) The mammalian passenger protein TD-60 is an RCC1 family member with an essential role in prometaphase to metaphase progression. Dev Cell 5:295–307
43. Li R (2007) Cytokinesis in development and disease: variations on a common theme. Cell Mol Life Sci 64:3044–3058
44. Bass MD, Morgan MR, Roach KA, Settleman J, Goryachev AB, Humphries MJ (2008) p190RhoGAP is the convergence point of adhesion signals from alpha 5 beta 1 integrin and syndecan-4. J Cell Biol 181:1013–1026
45. Elfenbein A, Rhodes JM, Meller J, Schwartz MA, Matsuda M, Simons M (2009) Suppression of RhoG activity is mediated by a syndecan 4-synectin-RhoGDI1 complex and is reversed by PKCalpha in a Rac1 activation pathway. J Cell Biol 186:75–83
46. Bass MD, Roach KA, Morgan MR, Mostafavi-Pour Z, Schoen T, Muramatsu T, Mayer U, Ballestrem C, Spatz JP, Humphries MJ (2007) Syndecan-4-dependent Rac1 regulation determines directional migration in response to the extracellular matrix. J Cell Biol 177:527–538
47. Yasui Y, Amano M, Nagata K, Inagaki N, Nakamura H, Saya H, Kaibuchi K, Inagaki M (1998) Roles of Rho-associated kinase in cytokinesis; mutations in Rho-associated kinase phosphorylation sites impair cytokinetic segregation of glial filaments. J Cell Biol 143:1249–1258
48. Minoshima Y, Kawashima T, Hirose K, Tonozuka Y, Kawajiri A, Bao YC, Deng X, Tatsuka M, Narumiya S, May WS Jr, Nosaka T, Semba K, Inoue T, Satoh T, Inagaki M, Kitamura T (2003) Phosphorylation by aurora B converts MgcRacGAP to a RhoGAP during cytokinesis. Dev Cell 4:549–560